IOP Conf. Series: Materials Science and Engineering **257** (2017) 012072 doi:10.1088/1757-899X/257/1/012072

Weld bead profile of laser welding dissimilar joints stainless steel

Ghusoon R Mohammed[1,2*], M Ishak[1], S N Aqida[1] and Hassan A Abdulhadi[1,2]

[1]Faculty of Mechanical Engineering, University Malaysia Pahang, Pekan 26600, Pahang, Malaysia
[2]Middle Technical University, Baghdad, Iraq

*Corresponding author email: ghusoon_ridha@yahoo.com

Abstract: During the process of laser welding, the material consecutively melts and solidifies by a laser beam with a peak high power. Several parameters such as the laser energy, pulse frequency, pulse duration, welding power and welding speed govern the mode of the welding process. The aim of this paper is to investigate the effect of peak power, incident angle, and welding speed on the weld bead geometry. The first investigation in this context was conducted using 2205-316L stainless steel plates through the varying of the welding speed from 1.3 mm/s to 2.1 mm/s. The second investigation was conducted by varying the peak power from 1100 W to 1500 W. From the results of the experiments, the welding speed and laser power had a significant effect on the geometry of the weld bead, and the variation in the diameter of the bead pulse-size. Due to the decrease in the heat input, welding speed affected penetration depth more than bead width, and a narrow width of heat affected zone was achieved ranging from 0.2 to 0.5 mm. Conclusively, weld bead geometry dimensions increase as a function of peak power; at over 1350 W peak power, the dimensions lie within 30 µm.

1. Introduction

In the critical industrial technologies, stainless steel is a vital material owing to its fine and excellent mechanical characteristics. Recently, many methods have been adopted by the researchers to improve further on the surface or total performance of steels to make it as fit as possible against any forms of severe conditions [1-3]. In addition, when joining stainless steel plates, it is necessary that most requires are achieved. One of the most common ways of joining materials is welding. Over the years, the welding of dissimilar metals has attracted much investigation interests; their increasing interest been justified by their economic and technical potentials. The idea of joining dissimilar metal has made it possible to achieve flexible product designs through an efficient use of each component material, (maximally utilizing the good specific attributes of individual material). The welding of dissimilar metals or alloys confers flexibility to the design but this often results in problems that have a negative impact on the weld performance [4].

There is a chance of failure of dissimilar welds which were performed on alloys with a wide thermal expansion coefficients variation either at the fusion zone (FZ), solidification, or during the service life of the product as a result of thermal fatigue [5, 6]. The joining of two metals with wide variation in their melting temperature or thermal conductivities is challenging because of the possibility of the material melting at different temperatures [7].

To control these problems, there is a need for a proper choice of the welding process. One of the most common methods of metal joining is the fusion welding. There have been continuous efforts to adopt these methods when joining dissimilar metals. Based on the temperature-pressure combination

of the individual metals, several welding processes such as arc welding, gas welding, solid-state welding, resistance welding, thermo-chemical welding and high energy beam welding have been developed. These welding processes produce different weld bead profiles and angular distortions to the weld pieces, as governed by the inherent characteristics of the process and the processing parameters.

Out of the whole welding processes, the high-energy beam welding process which uses a laser is more beneficial in terms of faster cooling rate, localized heating, less heat affected zone, and ease of access to the weld seam through fiber delivery, facilitating the welding of intricate geometries [8]. It often results in minimized distortion of the workpieces and the surface profile of the weld bead in controlled and ambient environments [9-11].

The adoption of heating sources with high-power density such as laser beam or electron beam can minimize some of these issues, owing to the greater monitoring of the shape and dimensions of the molten region and beam alignment; the high-power density allows for the immediate fusion of metals even when the melting temperatures vary. Many studies have reported the effect of fusion welding of materials that are characterized by different thermal, optical, electrochemical, and mechanical properties [12-14].

A careful selection of process parameters and requirements determines the successes of laser welding. A pre-knowledge of the expected temperature rise of the material is required when heating sheet metals with a laser beam. The increase in temperature can affect the geometry, velocity, workpiece hardness, gas flow rate, and microstructure of the weld piece. Many studies have investigated and estimated the geometry, hardness, heat affected zone, and microstructure of the weld beads.

The power of the laser beam and the welding speed have been reported as the major parameters that affect the penetration depth and bead width [15, 16]. The most significant parameter effect can lead to a weld with acceptable quality and efficiency. Lee et al have characterized the depth of the higher fusion zone to the width ratio, the cooling rate and the amount of porosity during welding using laser beam by varying the welding power, speed and focal position [17]. Similarly, the impact of different inert gases on the appearance of the weld line, the fusion zone dimensions, microhardness, solute evaporation, post weld tensile properties, and the porosity distribution has also been investigated. The increasing of the heat input, the area of the fusion zone, and the ratio of the dimensions of the weld area was shown to have an increasing trend. Paleocrassas [18] studied and reported the maximum welding speed as between 2 and 3 mm/s for a maximum penetration of 1.02 mm through the defining of the effluence and weld energy per weld length, considering the power, focal length and speed. The effect of the angle of incidence on the penetration depth, bead width and length have been investigated by Liao and Yu [19]. The study found reported an increase in the penetration depth and bead width and decreases in bead length when the incident angle was increased.

The width of the weld and penetration depth are the weld bead characteristics lengths that determine the cross section of the weld and with them, the strength or the shearing force of the weld joint can be determined [20-22]. Due to this, it is crucial to attain the right weld length characteristics. The fabricated weld geometric parameters must satisfy the requirements of the design and remain constant through the entire seam to achieve the performance desired from the weld joint in service. Therefore, in this paper the effect of welding speed, laser incident angle and the peak power on the weld bead dimensions (weld width and depth) and of the fusion zone welding will be presented.

2. Experimental details

The laser welding was studied in this report using a pulse wave fiber laser with an output power of 2 kW (Figure 1). A refractive optics based on focusing head with a focal length of 150 mm was used to direct the laser beam on the substrate. To avoid back reflection, the focusing head was tilted by 10° to the vertical axis. The surface of the workpieces was shielded with argon gas at the flow rate of 20 L/min. The austenitic stainless steel type (AISI316L) and duplex (AISI2205) which are some of the most common weld materials was used in this study. The materials used and their chemical composition and mechanical properties are shown in Tables 1 and 2.

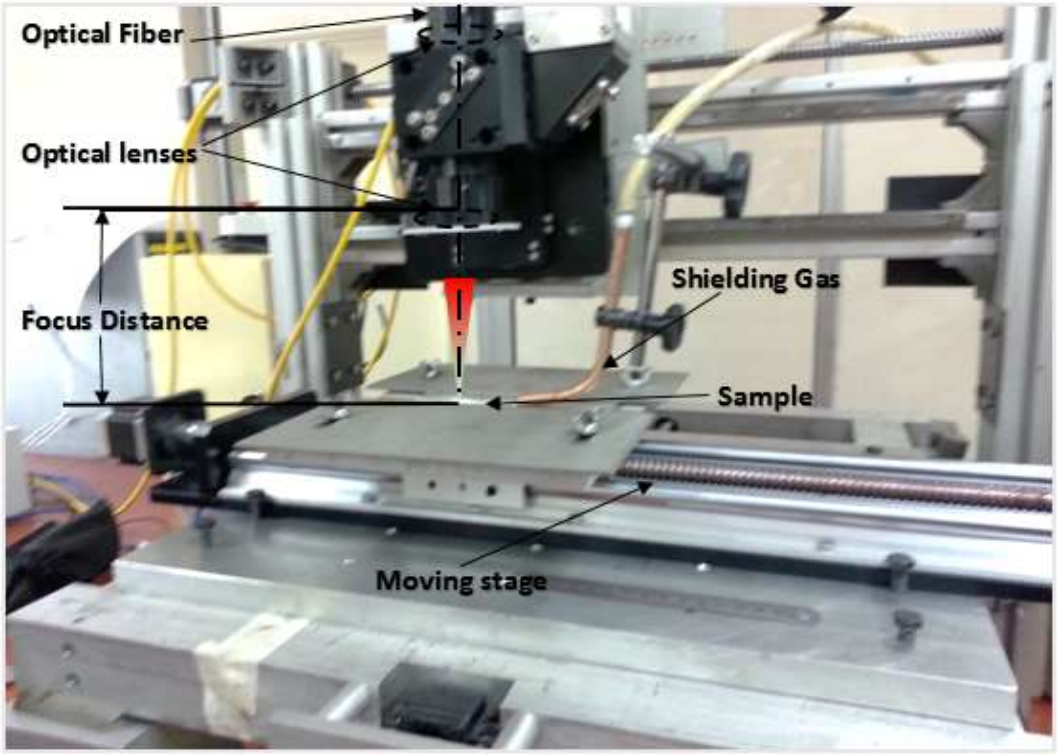

Figure 1. The set up for the fiber laser welding.

Table 1. The chemical composition of the base metal AISI 316L (wt. %).

Elements	C	Cr	Ni	Mn	Si	P	S	Mo	Nb
Weight (%)	0.03	16.5	9.6	1.15	0.48	0.003	0.005	2.4	0.002

Table 2. The chemical composition of AISI 2205 (wt. %).

Elements	C	Cr	Ni	Mn	Si	P	S	Mo	Nb
Weight (%)	0.03	22.07	4.8	1.15	0.53	0.003	0.005	3.65	0.002

To identify the process parameters for the laser welding, the laser power at 2 kW butt weld experiments were performed at different welding power and speeds; the plates were transversely cut towards the path of the laser beam propagation, and the cross section of the beam was examined under an optical microscope. The achieved aspect ratio (weld depth to width) of the weld bead cross-section was used for the selection of the optimum weld parameters based on the depth of penetration and minimal weld bead width. After this, the samples were prepared with the dimension of size 100 mm x 75 mm and thickness 2 mm, having square edges. The sketch of weld bead dimensions and the prepared samples is shown in Figure 2 and Figure 3, respectively.

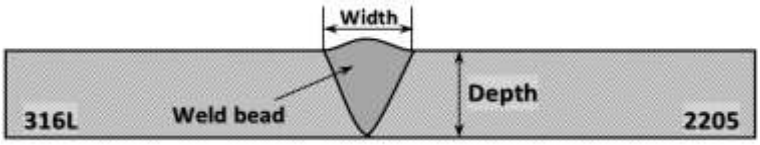

Figure 2. Sketch show the weld bead dimensions.

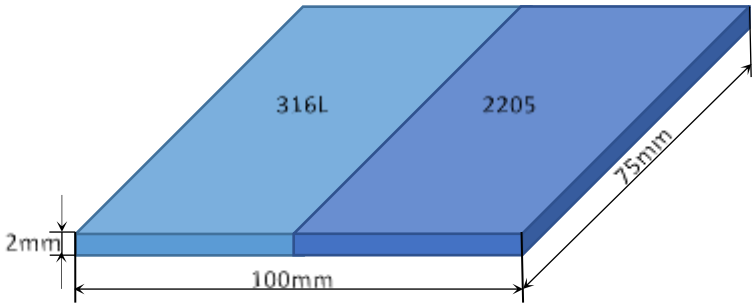

Figure 3. The sketch of the prepared samples.

The experiments for the welding were performed to investigate the effect of the welding speed, incident angle and peak power on geometry of the weld bead by varying the speed from 1.3 mm/s to 2.1 mm/s, the peak power from 1100 W to 1500 W, and the incident angle from 10° to 20°. The weld samples were transversely cut and the cross-sectional surfaces prepared for metallographic investigation. Different grades of polishing papers were used to polish the weld joints before etching with modified Kalling's regent to observe for the geometry of the weld bead. The prepared samples for metallographic investigation are shown in Figure 4 (a) to Figure 4(e), and Figure 5 (a) to Figure 5 (e). An optical microscope and image analyzer were used to measure the geometry of the weld bead parameters. Figure 6 shows the different zones of the 316L-2205 weld joints.

The heat affected zones of the weld samples were examined and found not to be in a straight line along the direction of the weld. This was because the base materials were non-homogeneous, as well as the power fluctuation and machine process capabilities.

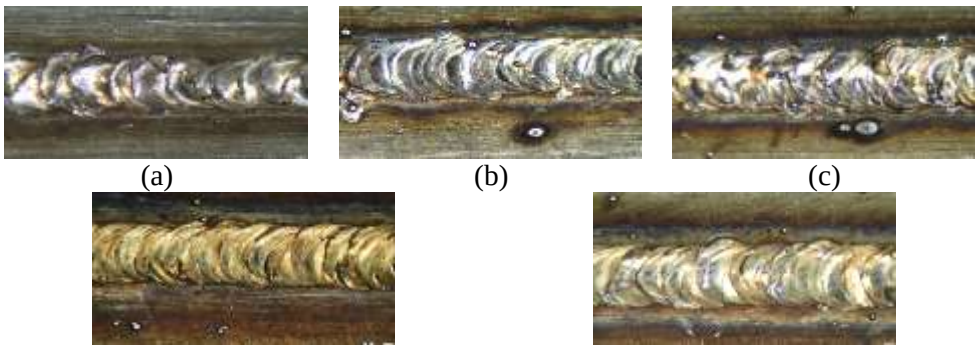

Figure 4. Top views of welded joints at welding speed. (a) 1.3 mm/s (b) 1.5 mm/s(c) 1.7 mm/s (d) 1.9 mm/s (e) 2.1 mm/s

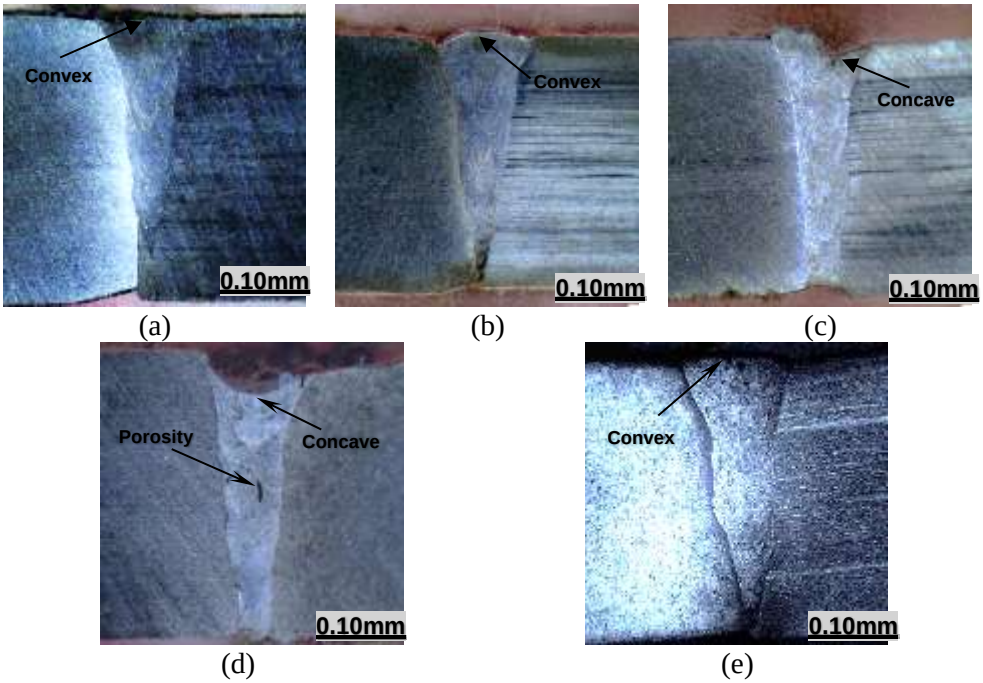

Figure 5. Transverse cross section of welded joints at welding speed. (a) 1.3 mm/s (b) 1.5 mm/s (c) 1.7 mm/s(d) 1.9 mm/s (e) 2.1 mm/s

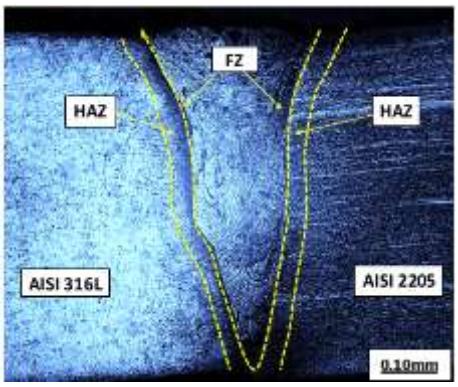

Figure 6. Micrograph of the different zones of the dissimilar welded joint.

Table 3. Parameters of fiber laser welding process.

Parameters	Values				
Peak power (W)	1100	1250	1350	1450	1500
Speed (mm/s)	1.3	1.5	1.7	1.9	2.1
Pulse width (ms)	3	4	5	6	6
Pulse repetition rate (Hz)	9	11	11	12	12
Incident angle	10°	12°	15°	18°	20°
Beam diameter (mm)	0.37	0.37	0.37	0.37	0.37
Laser energy density (W/mm^2)	10.4	11.8	12.7	13.7	14.1

3. Results and discussion

3.1. Effect of welding speed on weld bead profile

The surface changes of the welded pool were convex or concave in shape during the fusion welding. Few studies have investigated the mechanisms that are responsible for the shape of weld bead profile [23, 24]. In Figure 7, it was shown that the bead width and penetration depth depends on the weld speed as they decrease with increase in the welding speed.

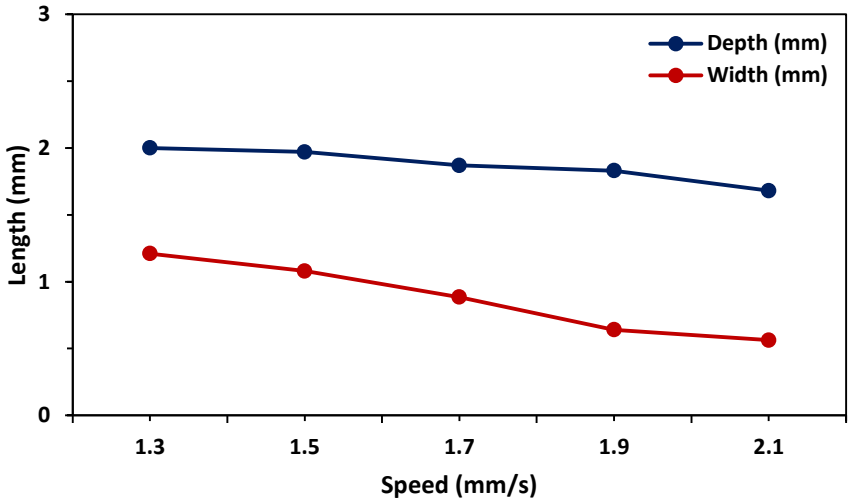

Figure 7. Effect of welding speed on bead width and depth of penetration of the welded joints.

The results suggested that the penetration depth depends more on the welding speed than the bead width due to the decrease in the heat input as well as less time of interaction between the source of the laser beam and the weld material. The weldment was found to be V-shaped, indicating the occurrence of the laser weld in keyhole mode [25, 26]. A narrow width of HAZ was achieved ranging from 0.2 to 0.5 mm and the width decreased as the welding speed increased.

The porosity of the welds was observed at some isolated locations, especially at the tip of the keyhole while welding at a lower speed due to the trapped gas [27] as shown in Figure 5d. At a higher speed, no porosity was observed. These observations agreed with the earlier reports [28, 29]. It was noted that the penetration depth is always greater than bead width in all consecutive spots due to the variation in the incident angle of the laser beam and the high heat input [19, 30].

3.2. Effect of peak power on weld bead profile

The dimensions of the weld pool were measured using image analyser. The geometry photographs of the weld pool created by the supply of pulse laser power input of 1100 W, 1250 W, 1350 W, and 1500 W with incident angle 20° are shown in Figure 8. The photographic inspection revealed an increase in the power input, leading to an increase in the dimensions of the weld bead and promoting spattering. In welding, spattering results in the reduction of the weld joint strength [31].

Figure 8 showed the bead width and penetration depth to depend on the peak power. As these values indicates, an increase in the heat input proportionately increases the bead width and penetration depth of the joints. For the HAZ area, a similar trend was followed with each of the associated joints. A similar trend has been reported by Yan [32] and Jana [33] while investigating TIG welded 304 SS and SMAW welded duplex SS, respectively. They found that an increase in the heat input increases the fusion zone and HAZ area. The size of the bead width and bead depth increased over a peak power range of 1100 -1500 W, and beyond 1350 W, the fluctuation in the weld bead geometry dimensions lied within 30 µm.

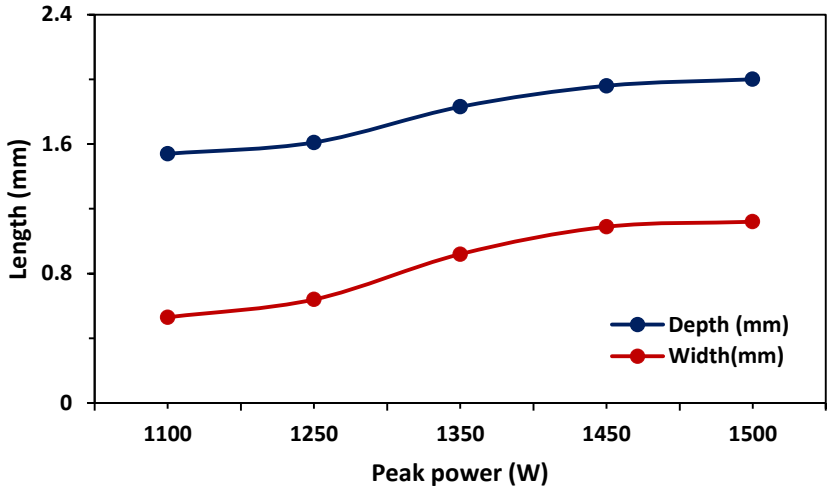

Figure 8. Effect of peak power on bead width and depth of penetration of the welded joints.

3.3. Effect of incident angle on weld bead profile

Figure 9 showed the depth of penetration to increase with increases in the incident angle at the laser energy range of 1100 - 1500W. The bead width, however, decreased with increase in the angle of incidence. Figure 9 also showed that the penetration depth and bead width are relatively short when the laser peak power (P.P) was 1100W.

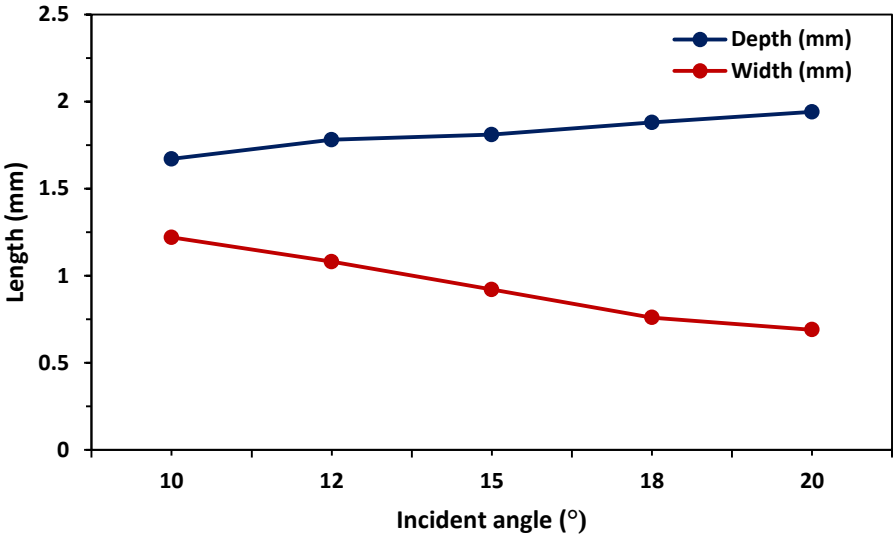

Figure 9. Effect of incident angle on bead width and depth of penetration of the welded joints.

The top view of the associated cross-sectional welded spot is presented in Figure 10 (a and b). The small depth of penetration and bead length were due to the low power density of the laser 967 W/mm^2 (<10^3 W/mm^2). When irradiated at this low density, the welding process is mainly conductive in nature [34, 35]. The keyhole welding which leaves a larger welding spot can occur only at a power density of more than 2×10^3 W/mm^2 since the laser power is not enough to cause boiling and hence, generate a keyhole [36]. The influenced zone in the specimen was basically caused by the conductive heat transfer, and the depth of penetration is limited (Figure 10b).

(a) (b)

Figure 10. (a) Top views of seam laser welded and (b) Metallographic of a cross-sectional specimen. Laser weld parameter: laser incident angle=10◦ and laser peak power =1100 W

4. Conclusions

From the experimental outcomes of the fiber laser welding process to joint dissimilar stainless steel plates, the following conclusions may be concluded:

1. There was a decrease in the fusion zone depth and width with increasing welding speed.
2. The width of the zone affected by heat is very narrow, ranging from 0.2 to 0.5 mm and decreases with increasing welding speed.
3. There was no solidification crack in the fusion zone, though porosity was seen occasionally.
4. The elevation in the laser energy promote the characteristic lengths of the penetration depth (D), and the bead width (W) as the laser beam incident angle increased.
5. The characteristic length of the bead width and weld penetration depth at the same laser beam incident angle increases with an increase in the laser energy.
6. The bead width variation was found to be very minimum and not significantly affected by the beam power, welding speed, and beam angle.
7. The characteristic lengths of the weld bead and the shape depend not only on the welding speed but also on the peak power and the laser beam angle of incidence.
8. A proper use of parameters during fibre laser welding in the industries can enhance the quality of weld joints and prolong the durability of finished products.

Acknowledgements

The authors wish to acknowledge the financial support provided by the Universiti Malaysia Pahang (UMP)-FKM under grant no. RDU150378 and GRS 1503107.

References

[1] Zhang K M and Zou J X 2012 *Thin Solid Films* **526** 28-33.
[2] Liu R L and Yan MFF 2010 Surf. Coat. Technol. 204 2251-6.
[3] Wickström L and Hinds G, Turnbull A 2015 *Corrosion* **71** 1036-47.
[4] Shah L H and Ishak M 2014 *Mater. Manuf. Process.* **29** 928-33.
[5] Lee H Y, Lee S H, Kim J B and Lee L H 2007 *Int. J. Fatigue* **29** 1868-79.
[6] Paventhan R, Lakshminarayanan P R and Balasubramanian V 2011 *Mater. Des*.**32** 1888-94.
[7] Velu M and Bhat S 2015 *Mater. Des.* **67** 244-60.
[8] Mohammed G R, Ishak M, Aqida S N and Abdulhadi H A 2017 *MATEC Web Conf.* **90** 01024.
[9] Nosyrev N A 2016 *Int. Conf Laser Opt.* (LO) S1-30-S1-.
[10] Katayama A, Kawahito Y and Mizutani M 2012 *Physics Procedia* **39** 8-16.
[11] Cui C, Cui X, Ren X, Liu T, Hu J and Wang Y 2013 *Mater. Des.* **49** 761-5.
[12] Tomashchuk I, Sallamand P, Belyavina N and Pilloz M 2013 *Mater. Sci. Eng. A-Struct. Mater.* **585** 114-22.
[13] Devendranath R K, Singh A, Raghuvanshi S, Bajpai B, Solanki T, Arivarasu, M 2015 J. Manuf. Process **19** 212-32.
[14] Romoli L and Rashed C A A 2015 Int. J. Adv. Manuf. Technol. **81** 563-76.

[15] Balasubramanian K R, Buvanashekaran G, and Sankaranarayanasamy K 2010 CIRP *J. Manuf. Sci. Technol.* **3** 80-4.
[16] Mohammed G R, Ishak M, Aqida S N and Abdulhadi H A 2017 *Metals* **7** 39.
[17] Lee M F, Huang J C, and Ho N J 1996 *J. Mater. Sci.* **31** 1455-68.
[18] Paleocrassas A G 2009 North Carolina State University.
[19] Liao Y C and Yu M H 2007 *J. Mater. Process. Technol.* **190** 102-8.
[20] Khan M A A, Romoli L, Fiaschi M, Dini G and Sarri F 2011 *Opt. Laser Technol.* **43** 158-72.
[21] Khan M A A, Romoli L, Fiaschi M, Sarri F and Dini G 2010 *J. Mater. Process. Technol.* **210** 1340-53.
[22] Khan M A A, Romoli L, Ishak R, Fiaschi M, Dini G and De Sanctis M 2012 *Opt. Laser Technol.* **44** 1611-9.
[23] Thomy C, Seefeld T and Vollertsen F 2008 *Weld World* **5** 9-18.
[24] Zhou J, Tsai H L and Wang P C 2005 *J. Heat Transf.-Trans. ASME* **128** 680-90.
[25] Fabbro R 2010 J. Phys. D-Appl. Phys. **43** 445501.
[26] Khan M A A, Romoli , Fiaschi , Dini G and Sarri F 2012 *J. Mater. Process. Technol.* **212** 856-67.
[27] Sales A M, Westin E M and Jarvis B L 2017 *Weld World*
[28] Katayama S, KawahitoY and Mizutani M 2010 *Physics Procedia* **5** 9-17.
[29] Kawahito Y, Matsumoto N, Abe Y, Katayama S 2013 *Weld Int.* **27** 129-135.
[30] Manonmani K, Murugan N, Buvanasekaran G 2007 *Int. J. Adv. Manuf. Technol.* **32** 1125-1133.
[31] Vasantharaja P, Vasudevan M and Maduraimuthu V 2017 *Trans. Indian Inst. Metals.*
[32] Yan J, Gao M and Zeng X 2010 *Opt. Lasers Eng.* **48** 512-517.
[33] Jana S 1992 *J. Mater. Process. Technol.* **33** 247-61.
[34] Curcio F, Daurelio G, Minutolo F M C and Caiazzo F 2006 *J. Mater. Process. Technol.* **175** 83-9.
[35] Triantafyllidis D, Schmidt M J J and Li L 2003 *J. Mater. Process. Technol.* **138** 102-8
[36] Li S, Chen G, Zhang Y, Zhang M, Zhou Y and Deng H 2014 *Laser Phys.* **24** 106003.